AIAA JOURNAL
Vol. 32, No. 1, January 1994

Vortex Distortion During Vortex-Surface Interaction in a Mach 3 Stream

Iraj M. Kalkhoran*
Polytechnic University, Brooklyn, New York 11201

An experimental study has been conducted in a Mach 3 wind tunnel to investigate the behavior of supersonic vortices as they interact with a wedge surface placed in their passage. The experimental setup was arranged so that interactions resulted in a close encounter of the vortex core and the wedge leading edge. Spark shadow photographs of the flowfield along with pressure measurements on the wedge surface were used to study the interaction problem. In their most organized form, distortion of streamwise vortices upon interacting with the wedge was found to result in formation of symmetric detached shock fronts far upstream of the wedge leading edge followed by an apparent slip surface separating a subsonic region from a supersonic zone. Interaction experiments leading to substantial changes in the structure of vortices revealed that the supersonic vortex distortion has strong resemblances to the incompressible "B-breakdown" reported in the literature. Experimental results also indicate that the interaction strongly depends on the vortex strength and vortex proximity to the wedge leading edge, and the generated flowfield was found to be highly unsteady. Interaction of concentrated streamwise vortices with the oblique shock formed over the wedge surface resulted in formation of a locally three-dimensional shock wave with a limited subsonic region downstream of the shock.

Nomenclature

Cp	= pressure coefficient, $(p-p_\infty)/q_\infty$
c	= airfoil chord
H	= enthalpy
h	= distance between the airfoil leading edge and the vortex generator tip, Fig. 2
L	= characteristic length
M	= Mach number
p	= pressure
q	= dynamic pressure
Re	= Reynolds number
s	= entropy
T	= temperature
t	= time
V	= velocity
x, y, z	= Cartesian coordinates
α	= vortex-generator angle of attack
Γ	= circulation

Subscripts

t	= tangential
VG	= vortex-generator
0	= stagnation condition
1	= condition ahead of the shock
2	= condition behind the shock
∞	= freestream

Introduction

UNDERSTANDING the dynamics and behavior of streamwise vortices is an important yet challenging task in the design of aerospace vehicles. At sufficiently high angles of attack, the vortex sheet generated by sharp leading-edge wing sections or the vorticity field found near the tip section of lifting surfaces roll up into organized concentrated vortices that convect downstream and may interact with other components of the vehicle. Such interactions may occur as a result of canard-shed vortices striking wing or aft control surfaces of an aircraft or as a result of forward fin/body shed vortices interacting with aft control surfaces in a missile. In general, these interactions are three dimensional and unsteady, and they may lead to a loss of lift, an increase in drag, and sudden changes in the pitching moment characteristics of the vehicle, thus limiting maneuverability and influencing stability and control characteristics. Beyond a critical angle of attack, vortices formed over highly swept sharp leading edges are known to undergo a drastic change in structure in a phenomenon called "vortex breakdown" or "vortex bursting."[1-5] It is also well established that vortex breakdown in incompressible flows may occur, for example, if streamwise vortices are subjected to sufficiently strong adverse pressure gradients. The vortex breakdown phenomenon cited in the low-speed literature is in general characterized by a sudden growth of the vortex size followed by a region of highly turbulent flow and formation of local stagnation zones and regions of reversed axial flow.

The vortex breakdown phenomenon of low-speed flows has been examined by several investigators, and comprehensive surveys of vortex breakdown are presented by Hall,[6] Benjamin,[7] and Leibovich.[8] Leibovich,[8] for example, describes vortex breakdown to be a discontinuous transition between two flows with very different characteristics: a supercritical region incapable of admitting upstream propagating waves and a subcritical state that admits upstream propagating waves. In a sense, such a description of the vortex breakdown is reminiscent of normal shocks in gasdynamics.[8] An interesting aspect of this description of vortex breakdown involves passing a streamwise vortex through a shock wave. Interaction of a vortex with a normal shock wave always results in a supercritical (supersonic flow ahead of the shock) to subcritical (subsonic flow behind the shock) transition, whereas crossing a vortex through an oblique shock wave does not necessarily involve a supercritical to subcritical transition. The two types of shock wave/vortex interactions are schematically shown in Fig. 1.

Although the vortex breakdown phenomenon in supersonic flows has been examined by a few investigators, the problem has only recently attracted serious consideration. Previous numerical and experimental studies relevant to the vortex breakdown phenomenon in supersonic flows have mainly concentrated on investigating the behavior of streamwise vortices as a result of a shock wave/vortex interaction, and attempts have been made to develop a vortex breakdown criterion based on vortex swirl rate and shock wave strength.[9,10] Moreover, such studies have been mainly limited to interaction of streamwise vortices with normal shock waves. On the numerical side, a few contributions have dealt with

Received July 15, 1992; presented as Paper 93-0761 at the AIAA 31st Aerospace Sciences Meeting, Reno, NV, Jan. 11–14, 1993; revision received June 14, 1993; accepted for publication June 25, 1993.

*Assistant Professor, Aerospace Engineering Department. Member AIAA.

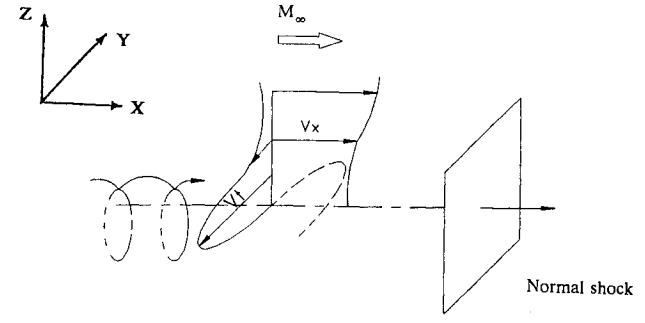

a) Normal shock wave/vortex interaction

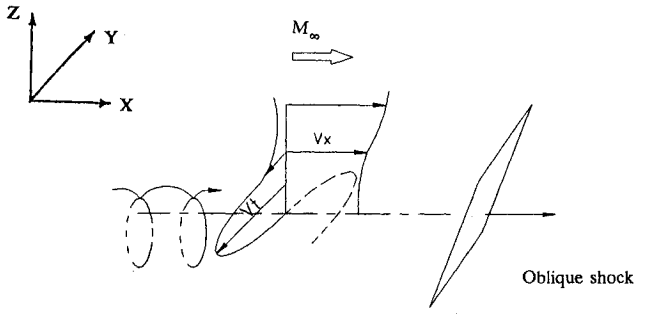

b) Oblique shock wave/vortex interaction

Fig. 1 Normal and oblique shock wave/vortex interactions.

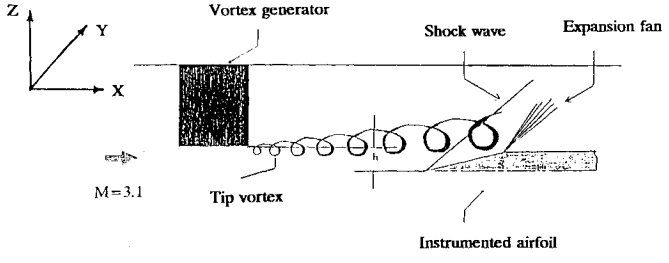

Fig. 2 Schematic of the experimental arrangement.

the behavior of vortices upon encountering an abrupt pressure jump imposed by shock waves. Unsteady Navier-Stokes calculations were performed by Kandil et al.[11] for the case of quasi-axisymmetric vortices interacting with normal shocks in an inlet-type configuration that revealed several vortex breakdown modes. Copening and Anderson[12] reported three-dimensional Euler solutions for the interaction of streamwise vortices with oblique shock waves at Mach numbers of 2.28 and 5.0 with no apparent vortex breakdown. On the other hand, regions of reversed flow as well as convex-concave shock shape were reported. Experimental studies of normal shock wave/vortex interaction were performed by Zatoloka et al.,[13] Delery et al.,[9] Metwally et al.,[10] and Cattafesta and Settles,[14] who all reported some form of vortex breakdown. References 9 and 10 also reported numerical predictions to substantiate the experimental observations. An experimental study of the interaction of wing-tip vortices with two-dimensional oblique shock waves, reported by Kalkhoran et al.,[15] indicated a deflection of the vortex in crossing oblique shock waves with no apparent vortex breakdown; however, such interactions were limited to relatively weak shock waves and vortices.

A dimensional analysis of the shock wave/vortex interaction problem indicates that the appropriate simulation parameters are the flow Mach number M_∞, Reynolds number Re, a shock wave strength parameter p_2/p_1, and a vortex intensity parameter defined by $\Gamma/V_\infty L$. Although the shock strength parameter defined by p_2/p_1 accounts for the pressure jump imposed on the vortex by the shock wave, a more appropriate parameter will include the shock inclination angle since, in addition to the shock strength, the vorticity jump across a shock wave is influenced by the shock curvature and the magnitude of the velocity component tangent to the shock.[16] For the case of an axisymmetric vortex frequently used in numerical modeling of vortex flows, the interaction of vortices with normal shocks in the absence of vortex breakdown is governed by the axial Mach number distribution in the vortex core and the flow condition downstream of the shock. On the other hand, the interaction of axisymmetric vortices with two-dimensional oblique shocks is influenced by both axial and tangential components of velocity, and downstream influences are not present during such encounters.

An important issue to be addressed in the study of the shock wave/vortex interaction problem is how the vortex and the shock wave mutually influence one another. To date, flow visualization taken during shock wave/vortex interactions experiments[10,13–15,17] with apparent vortex breakdown have indicated some form of a three-dimensional curved shock structure leading portion of which is normal to the axial flow direction with a limited region of subsonic flow downstream of the shock wave. These observations suggest that encounters, at least leading to drastic changes in the vortex structure, are affected by both the upstream and the downstream flow conditions. Furthermore, since a planar shock wave is only possible for uniform entropy distribution upstream of the shock, it is evident that introducing a concentrated vorticity field in an otherwise uniform flow ahead of a planar shock wave (oblique or normal shock) will result in a locally nonuniform flow upstream of the shock leading to some form of distorted shock pattern. Crocco's theorem for a steady inviscid flow is

$$T\nabla s = \nabla H_0 - \boldsymbol{V}\times(\nabla\times\boldsymbol{V})$$

which states that a vortex filament of limited spatial extent immersed in a uniform irrotational flow ahead of a planar shock wave will lead to nonuniform entropy distribution upstream of the shock, giving rise to the formation of a locally distorted curved shock structure. On the other hand, the behavior of vortices upon crossing shock fronts is not well understood at the present time. The present experimental study is aimed at understanding global aspects of behavior of streamwise concentrated tip vortices upon interacting with a wedge surface and gaining a better understanding of the vortex distortion in supersonic flows. In particular, emphasis is placed on detecting similarities and differences between supersonic and incompressible vortex breakdown phenomena.

Experimental Setup

Vortex-surface interaction studies were conducted in Polytechnic University's Mach 3 wind-tunnel facility.[18] The wind tunnel is a blowdown-type facility and has a 25.4 × 25.4 cm test section. The wind tunnel is capable of producing flow with a nominal Mach number of 3.1 and Reynolds numbers in the range of 6×10^7

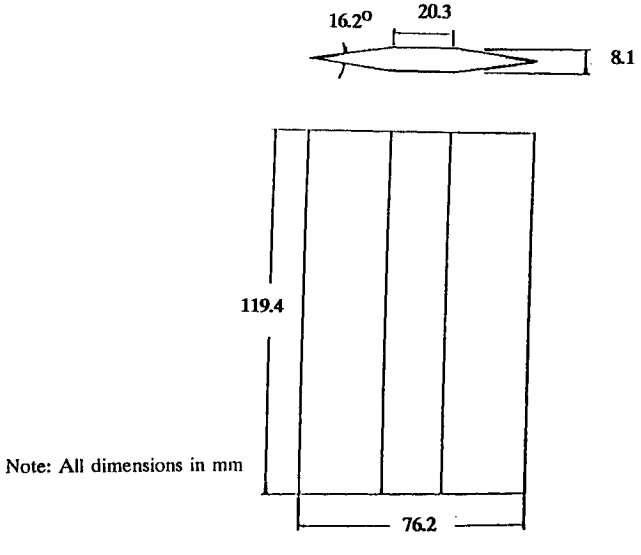

Fig. 3 Geometry of the vortex generator wing section.

to 16×10^7 per meter. The stagnation temperature and pressure for the present experiments were ambient and 1.2 MPa, respectively, resulting in a flow Reynolds number of 8.9×10^7 per meter. Figure 2 illustrates the schematic of the experimental arrangement. Tip vortices were generated by placing a lifting surface at positive angles of attack (trailing edge into the page in Fig. 2). The vortex generator was a semispan slender wing section having a maximum section thickness of 10%, a chord length of 7.62 cm, and a span of 11.94 cm (Fig. 3). The vortex generator was mounted on the test section ceiling at the tunnel centerline and extended vertically downward. With this arrangement, tip vortices with various strengths could be generated by placing the vortex generator at different angles of attack in the range $-10 < \alpha_{VG} < 10$ deg.

A two-dimensional shock generator having a wedge angle of 27 deg and a chord length of 3.81 cm (Fig. 4) was placed 15.7 cm (4.1 vortex-generator chord lengths) downstream of the vortex-generator wing section. The wedge section was capable of being traversed in the vertical direction so that the vortex height relative to the wedge leading edge could be adjusted. The wedge surface was equipped with 18 pressure taps at three equally spaced spanwise rows at $y/c = -0.13$, 0, and 0.13 ($y = 0$ is the wedge midspan location) and six equally spaced chordwise locations from $x/c = 0.13$ to $x/c = 0.80$ (Fig. 4). Further details of the experimental arrangement may be found in Ref. 17.

A possible drawback of using wing tip vortices to study shock wave/vortex interaction problems is that interference might occur due to the complex wave structure (shock or expansion waves) caused by the wing placed in a supersonic stream, thereby adversely influencing the flowfield ahead of the shock. However, the problem can be circumvented by placing the downstream surface such that strong disturbances (or their reflections from the tunnel walls) are behind the wedge surface. This was addressed in Ref. 15 where five-hole cone probe measurements indicated that outside of the vortex core the flow was essentially that of the freestream and

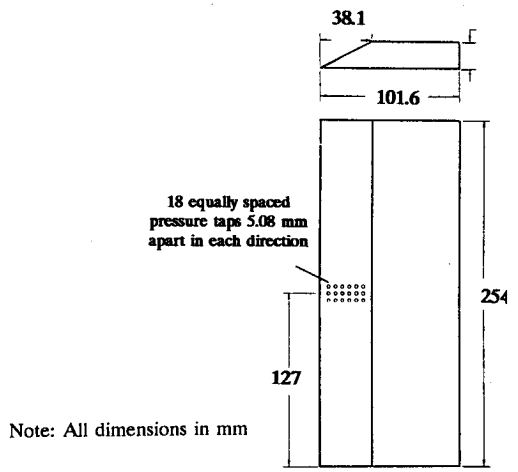

Fig. 4 Geometry of the 27-deg two-dimensional wedge section.

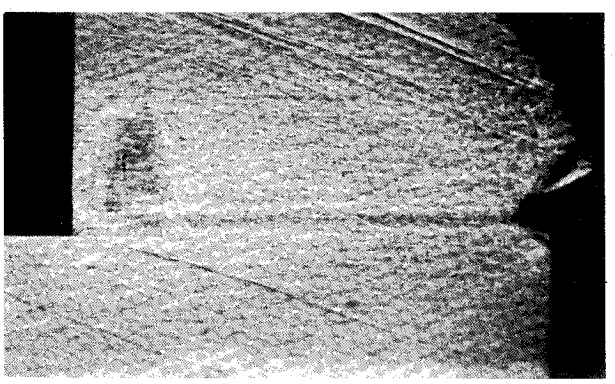

Fig. 5 Shadowgraph of the flowfield generated during the head-on interaction of the vortex and the wedge for $\alpha_{VG} = 5$ deg.

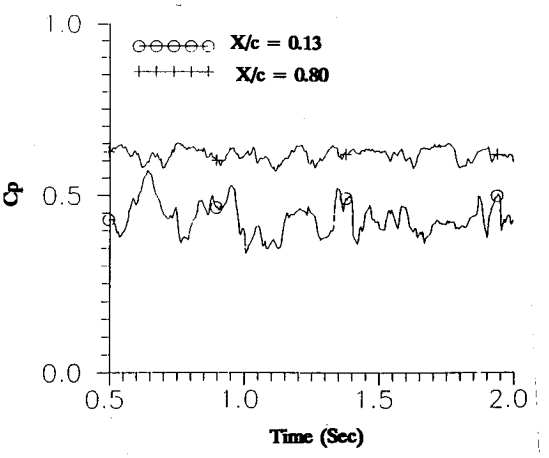

Fig. 6 Time history of the wedge pressure coefficient during the interaction for $\alpha_{VG} = 5$ deg.

the wave interference on the interaction for the present configuration was not significant.

Flow diagnostic techniques included simultaneous wedge surface pressure measurements and a multiple spark shadow photograph of microsecond spark duration. Typical wind-tunnel running times were 3 s, and pressure data at the rate of 250 Hz for a period of 2 s during the steady-state portion of a run were acquired. Interaction experiments were carried out for three vortex-generator angles of attack of $\alpha_{VG} = 5$, 7.5, and 10 deg for several vortex-wedge separation distances. Only the cases represented by the interaction for vortex-generator angles of attack of 5 and 7.5 deg during close encounters will be presented here. Details of the parametric study may be found in Ref. 17.

Results and Discussion

A typical spark shadowgraph of the flowfield during a head-on interaction of a relatively weak vortex with the wedge is shown in Fig. 5. The flow is from left to right, and the aft segment of the vortex generator may be seen in the upper left portion of the photograph. The wedge section is located at the lower right of the shadowgraph with the inclined portion of the wedge terminating exactly at the edge of the picture. The flowfield was generated by interaction of a tip vortex created by placing the vortex generator at an angle of attack of 5 deg. The picture clearly indicates a concentrated trailing tip vortex originating at the vortex-generator tip, convecting downstream, and intersecting the wedge surface with the vortex core very close to the airfoil leading edge. Extensive multiple spark shadowgraphs (generally four per run) taken during the encounter indicated an unsteady movement of the vortex core during the interaction process; thus the head-on collision of the vortex core and the wedge leading edge occurred only in a transient manner. Study of shadowgraphs similar to the one shown in Fig. 5 indicated only a slight modification to the wedge shock wave, whereas the main features of the flowfield appeared to remain unchanged.

Examination of the chordwise pressure distribution during the weak encounter ($\alpha_{VG} = 5$ deg) indicated an unsteady flow with relatively large amplitude pressure fluctuations as a result of the interaction. Figure 6 illustrates the time history of the pressure coefficients at two chordwise locations along the wedge surface for a period of 1.5 s. Although the use of finite length tubing from pressure ports to the pressure transducers does not permit time-accurate analysis of pressure traces, these trends provide certain information concerning mean characteristics of the interaction process. Two points concerning time history variation of the wedge pressure distribution are immediately obvious. First, higher amplitude pressure fluctuations are seen near the airfoil leading edge at $x/c = 0.13$ in comparison with pressure variations at $x/c = 0.80$. Second, on the average, higher vortex-induced suction pressures may be seen near the wedge leading edge than further downstream. Although shadowgraphs taken during the weak en-

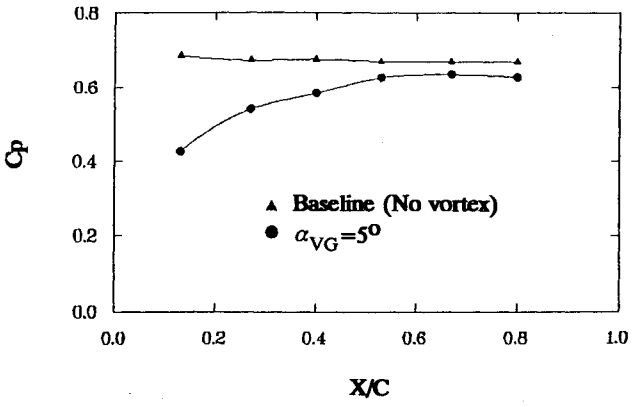

Fig. 7 Time-averaged chordwise pressure distribution during the interaction for $\alpha_{VG} = 5$ deg.

a) $t = 0.52$

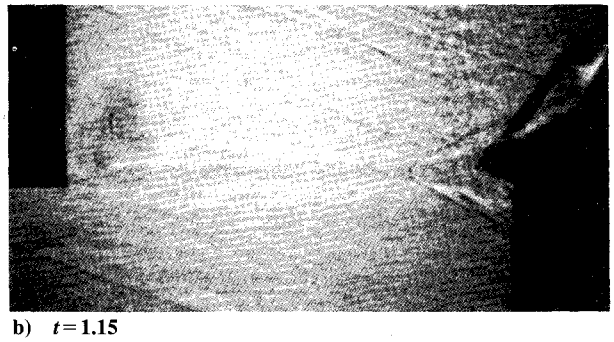

b) $t = 1.15$

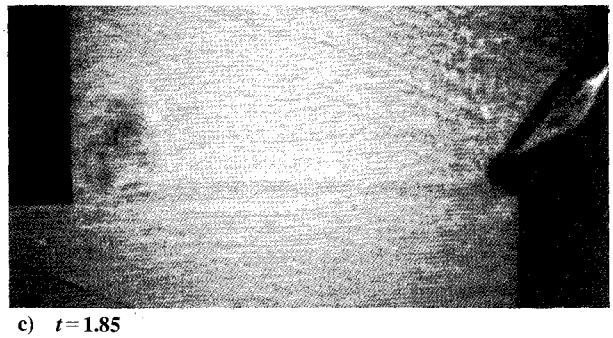

c) $t = 1.85$

Fig. 8 Shadowgraph of the flowfield generated during the head-on interaction of the vortex and the wedge for $\alpha_{VG} = 7.5$ deg.

counter represented by $\alpha_{VG} = 5$ deg did not reveal any major alteration of the flowfield in comparison with the stronger encounter to be discussed later (at least in the shadowgraph viewing area that includes the entire chord of the wedge section), pressure data similar to that shown in Fig. 6 suggest some form of vortex weakening with increasing chordwise distance as a result of the encounter. Time-averaged chordwise pressure coefficient distribution for the case represented by $\alpha_{VG} = 5$ deg is compared with the baseline pressure distribution in the absence of the vortex generator in Fig. 7, which verifies the aforementioned behavior.

Interaction experiments incorporating stronger tip vortices were carried out by placing the vortex generator at an angle of attack of 7.5 deg. Successive spark shadowgraphs of the flowfield during a typical run for this encounter are presented in Figs. 8a–8c. These figures show temporal shadow photographs taken at $t = 0.52$, 1.15, and 1.85 s, where $t = 0$ is approximately the wind-tunnel starting time. An unsteady movement of the vortex core may be seen by comparing Figs. 8a and 8c. Figure 8a clearly shows the vortex core passing over the wedge leading edge, whereas in Fig. 8c the vortex is seen to pass below the wedge leading edge. Figure 8b, on the other hand, represents a head-on collision of the vortex and the wedge leading edge as a result of which the formation of a "detached" shock upstream of the airfoil leading edge is observed. Be-

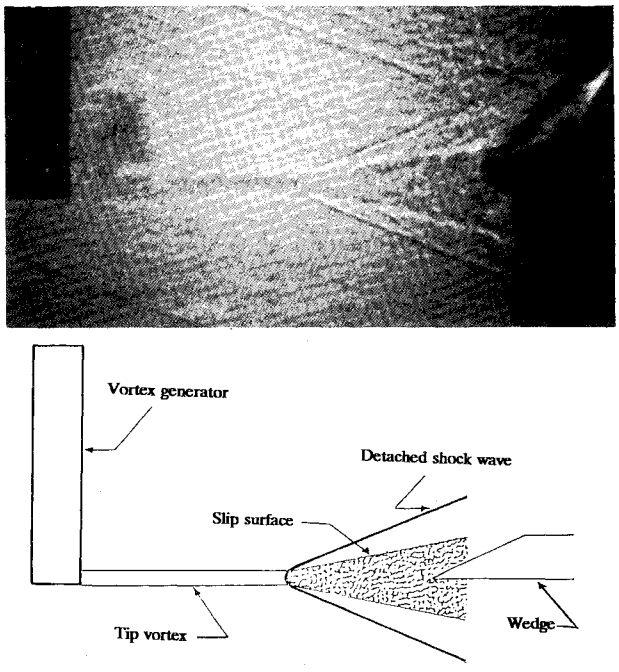

a) $t = 0.65$

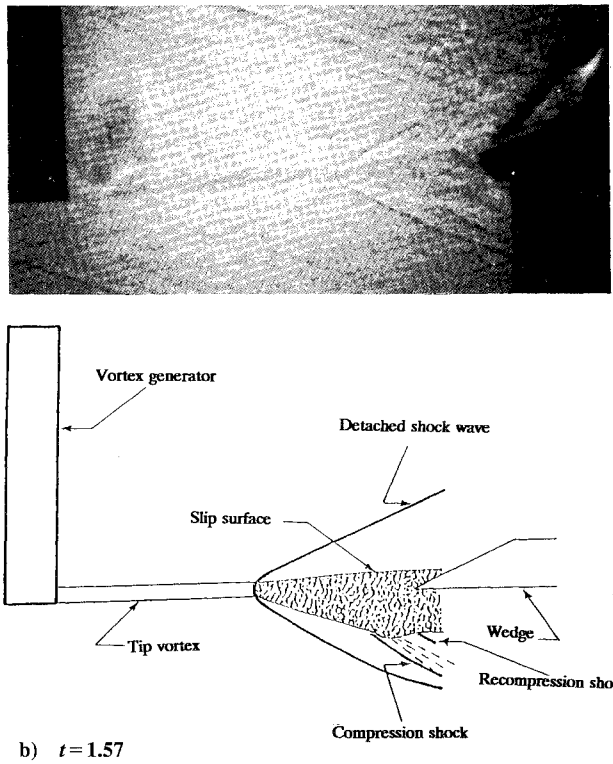

b) $t = 1.57$

Fig. 9 Shadowgraph of the flowfield generated during the head-on interaction of the vortex and the wedge for $\alpha_{VG} = 7.5$ deg.

hind the detached shock wave, the flow shown in Fig. 8b may be seen to consist of two distinct regions (also see, for example, Fig. 9): a central zone characterized by a darkly shaded conical region with its vertex situated at the vortex center and a lighter area between the shock and the central conical region. The detached shock wave is seen to be strongly curved in the vicinity of the vortex core, whereas outside of the vortex core the shock is straight. Behind the curved portion of the shock, the vortex grows in size to form a central conical region. The rapid radial expansion of the vortex core in crossing the detached shock wave may be seen to have a strong visual resemblance to the incompressible B-breakdown reported in the literature. Although the generated flowfield in this study leading to formation of these shock patterns occurred in a transient manner, the detached shock fronts were observed in all shadowgraphs taken during the head-on encounter of the vortex and the wedge leading edge.

Comparison of Figs. 8a and 8b reveals another important feature of the vortex-wedge interaction. These figures indicate that the encounter can lead to formation of a locally detached shock wave (Fig. 8b), which implies a local region of subsonic flow ahead of the wedge. This is similar to the flowfield downstream of a detached shock wave formed in front of a blunt body placed in a supersonic stream. Moreover, the leading portion of the detached shock is normal to the axial flow direction, and since the tangential velocity is negligible at the vortex center, the flow immediately downstream of the normal portion of the shock wave is necessarily subsonic.

The aforementioned behavior may be more clearly seen in the shadowgraphs of Fig. 9. Figure 9a taken at $t=0.65$ s clearly indicates both a fairly symmetric detached shock structure and a distinct symmetric boundary between the two regions, suggesting little mixing of the two flows. Again, the vortex may be seen to expand upon crossing the curved portion of the shock wave to form a well-defined boundary separating the central conical region from the outer flow. An interpretation of the photograph can also be seen in Fig. 9a. The distortion of supersonic vortices upon encountering a strong pressure jump, at least in their most organized form, consists of two distinct flow regimes (of different entropies) separated by a slip surface: a central subsonic region containing the distorted vortex structure and a supersonic outer region downstream of the straight portion of the detached shock wave. The subsonic conical region is formed as a result of vortex distortion and acts as a solid conical body for the supersonic incoming flow as a result of which a detached shock wave is formed. This shock wave bears a strong similarity to the shock wave formed over a conical surface placed in a supersonic stream with one notable exception, i.e., at the apex where the observed detached shock in the present problem has a strong curvature. This difference may be explained by the nonuniform vortex core Mach number distribution approaching the slip surface that forms in the region between the shock and the wedge. However, since the spatial extent of the vortex core is small in comparison to the outer irrotational flow, the main features of the flow leading to the formation of the detached shock wave are governed by the uniform freestream flow outside of the vortex core, and the presence of the vortex only modifies the leading portion of the shock wave. The generated flowfield may be seen to have striking similarities to the incompressible B-breakdown model that, as described by Leibovich,[8] resembles a body of revolution placed in the flow.

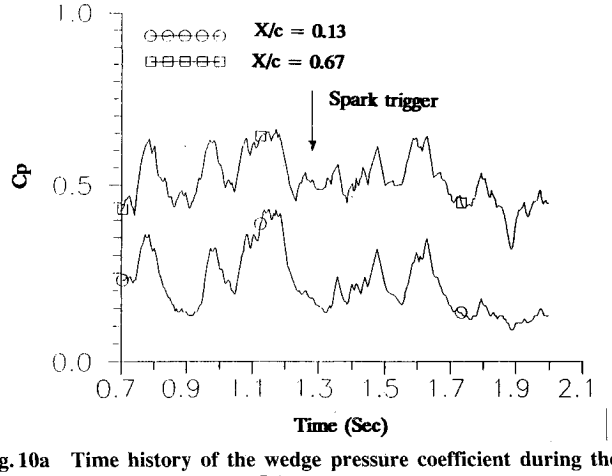

Fig. 10a Time history of the wedge pressure coefficient during the strong interaction for $\alpha_{VG}=7.5$ deg.

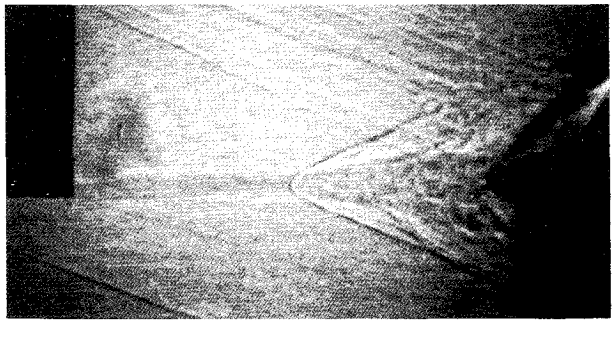

Fig. 10b Shadowgraph of the flowfield generated during the strong interaction at $t=1.28$ s.

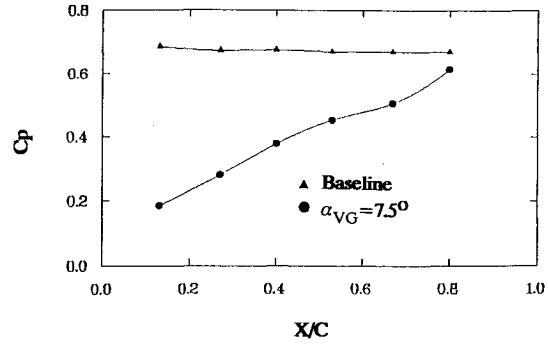

Fig. 11 Time-averaged chord wise pressure distribution during the head-on interaction of the vortex and the wedge for $\alpha_{VG}=7.5$ deg.

More insight into the problem may be gained by considering Fig. 9b taken at $t=1.57$ s that indicates a somewhat different shock structure with a slight deviation from a symmetric form (as indicated by the higher curvature of the lower portion of the shock wave). Moreover, the formation of compression and recompression shock waves may be noted in the neighborhood of the bulged-out portion of the detached shock. The formation of these shock waves is due to the local deformation of the slip surface as a result of which the outer supersonic flow is required to be deflected. Comparison of shadowgraphs shown in Figs. 9a and 9b also indicates an increase in the detached shock inclination angle in Fig. 9b, which may be seen to be due to a further expansion of the region containing the distorted vortex structure, thus an increase in the slip surface angle. The formation of subsonic and supersonic regions as a result of vortex distortion may also be verified by noting that the compression and recompression waves in Fig. 9b terminate at the slip surface and do not extend into the subsonic conical region. The flowfield generated by Fig. 9b is believed to mark the initial stages of detached shock disappearance as a result of unsteady movement of the incoming vortex leading to flowfields similar to those seen in Figs. 8a and 8c.

To further substantiate such arguments, the half-angle of the assumed slip surface was determined from the shadowgraph of Fig. 9a to be approximately 12.2 deg. Assuming a conical flow and a freestream Mach number of 3.1, the generated conical shock wave half-angle from Ref. 19 may be found to be 22.2 deg, which compares favorably with the measured shock angle of 22 deg. An explanation of this is given in the following manner. Upstream of the detached shock wave, the flowfield is composed of a rotational region within the vortex core and an irrotational uniform flow with a scale much larger than that of the vortex core diameter. This was illustrated in Ref. 15 where a five-hole cone probe survey of the

a) $t = 1.12$

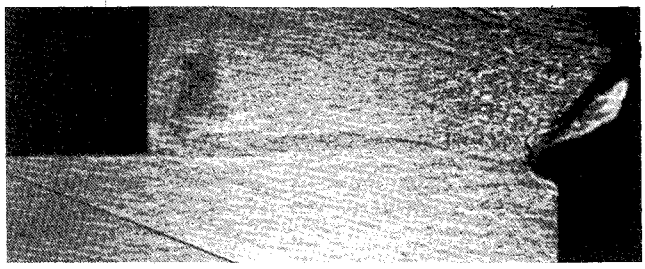

b) $t = 1.5$

Fig. 12 Shadowgraph of the flowfield generated during an oblique shock wave/vortex interaction for $\alpha_{VG} = 7.5$ deg.

vortex core indicated that the generated vortices have a viscous core diameter on the order of 0.2 chord (1.5 cm). Thus, it is reasonable to expect that the main features of the flow leading to the formation of detached shock waves will be governed by the irrotational freestream flow approaching the assumed surface. On the other hand, as already stated, the nonuniform Mach number distribution in the vortex core only influences the leading portion of the shock wave, whereas outside the vortex core it asymptotically weakens to a conical shock structure corresponding to the theoretical shock strength.

Another important aspect of the interaction is the mechanism behind generation of these detached shock waves. Although the exact cause of this phenomenon is not well understood at the present time, a candidate mechanism to explain this behavior is the inability of the wedge to support an attached shock wave as a result of the vortex core Mach number distribution. A detached shock may develop due to either low Mach number or high flow deflection angle created by vortex-induced flow angularity. This will result in the formation of a locally detached shock front leading portion of which is a normal shock wave with a subsonic flow just downstream. The strong pressure jump across the normal portion of this detached shock wave will then be responsible for the distortion of the vortex possibly in a manner similar to the subsonic vortex breakdown. Furthermore, the subsonic region just downstream of the normal portion of the shock will then justify further upstream propagation of the detached shock wave.

Additional information concerning the flowfield generated by the strong interaction may be gained by considering simultaneous shadowgraphs along with the wedge surface pressure data. Figure 10a shows the time history plot of the chordwise pressure distribution, and the shadow photograph taken at $t = 1.28$ s during the same run is shown in Fig. 10b. It should be noted that the spark trigger time for the shadowgraph as indicated in Fig. 10a has a time accuracy of 4 ms as determined by the data acquisition sampling frequency, whereas, as already mentioned, due to the use of finite tubing length, only an estimate of actual pressure variations with time could be gained from the time history plots. With these limitations in mind, a time average of the pressure coefficient distribution in the range of $1.25 < t < 1.45$ (50 data points) was used to construct the time-averaged pressure coefficient distribution and is compared with the baseline values in the absence of the vortex generator in Fig. 11. The aforementioned figure indicates that, similar to the weak interaction ($\alpha_{VG} = 5$ deg), the most pronounced vortex influence on the wedge pressure distribution is near the airfoil leading edge and that at distances further downstream the vortex influence on the wedge pressure distribution progressively decreases.

Interaction experiments with a vortex-wedge vertical separation distance of $h/c = 0.40$ (Fig. 2) resulted in encounters with the vortex passing over the wedge leading edge, thus creating an oblique shock wave/vortex interaction. It should be noted that the nondimensional separation distance parameter h/c is a reference geometric parameter defined by the distance between the vortex-generator tip and the wedge leading edge and in general does not represent the actual vortex height relative to the wedge leading edge. Instantaneous spark shadow photographs of the flow during an oblique shock wave/vortex interaction are shown in Figs. 12a and 12b at $t = 1.2$ and 1.5 s, respectively. These figures indicate a concentrated tip vortex convecting downstream that intersects the oblique shock wave formed over the wedge section. The interaction is generated by the vortex generator and the wedge section placed at angles of attack of 7.5 and 0 deg, respectively, with the resulting shock strength parameter $p_2/p_1 = 5.63$. From the shadowgraphs of Fig. 12, a highly turbulent region downstream of the shock wave, characterized by the darkly shaded area, may be seen. In comparing the two shadowgraphs, the most noticeable difference is the appearance of a bulged-forward shock structure in Fig. 12b situated slightly above and upstream of the wedge leading edge. Similar to the detached shock fronts observed during the head-on collision of the vortex and the wedge leading edge discussed earlier, the shock wave may be seen to have a strong curvature at the apex that is located at the vortex center. Comparison of Figs. 12a and 12b also indicates that the generated flowfield is unsteady, leading to temporal formation of a three-dimensional shock structure. Moreover, similar to the case leading to the formation of detached shock waves, the leading portion of the curved shock is normal to the axial flow direction at the vortex center, which suggests that a limited region of subsonic flow downstream of the curved portion of the shock exists.

Conclusions

The interaction of trailing tip vortices with a two-dimensional wedge surface during a close encounter was experimentally examined in a Mach 3 stream. The vortex strength and the vortex core proximity to the wedge leading edge were found to strongly influence the flowfield generated by the interaction. For interactions incorporating weak vortices ($\alpha_{VG} = 5$ deg), vortex distortion was not visually detected in the viewing area in the shadowgraphs, whereas the wedge pressure distribution indicated an alteration of the airfoil pressure distribution during the encounter. For the case of stronger vortices ($\alpha_{VG} = 7.5$ deg) interacting with the wedge surface, the interaction resulted in formation of unsteady detached shock fronts far upstream of the wedge leading edge. In their most organized form, distortion of concentrated streamwise vortices during a head-on encounter with the wedge leading edge were found to form a fairly symmetric slip surface separating a subsonic region from a supersonic zone with the subsonic region resembling a solid conical body placed in a supersonic stream. When the vortices intersected the oblique shock wave that formed over the wedge, the formation of a locally three-dimensional and unsteady shock structure was observed.

Acknowledgments

This work was partially supported by the Air Force Office of Scientific Research Grant F49620-93-1-0009 and NASA Lewis Research Center Grant NAG 3-1378. The author thanks Lester Orlick and Frank Wang for their assistance throughout this work. A debt of gratitude is owed to James Bentson for many valuable discussions and suggestions.

References

[1]Werle, H., "Sur l'eclatement des tourbillons d'apex d'une aile delta aux faibles vitesses," *La Recherche Aeronautique*, No. 74, Jan.–Feb. 1960, pp. 23–30.

[2]Jones, J. P., "The Breakdown of Vortices in Separated Flow," Rept. 140, Aeronautical Research Council, 22, 241, London, July 1960.

[3]Squire, H. B., "Analysis of 'Vortex Breakdown' Phenomenon," Imperial College of Science and Technology, Aeronautics Dept., Rept. 102, Part I, London, July 1960.

[4]Lambourne, N. C., and Bryer, D. W., "The Bursting of Leading-Edge Vortices—Some Observations and Discussion of the Phenomenon," Aeronautical Research Council, Rept. 3282, London, April 1961.

[5]Elle, B. J., "On the Breakdown at High Incidences of the Leading Edge Vortices on Delta Wings," *Journal of the Aeronautical Society,* Vol. 64, Aug. 1960, pp. 491–493.

[6]Hall, M. G., "Vortex Breakdown," *Annual Review of Fluid Mechanics,* Vol. 4, 1972, pp. 195–218.

[7]Benjamin, T. B., "Theory of the Vortex Breakdown Phenomenon," *Journal of Fluid Mechanics,* Vol. 14, Dec. 1962, pp. 593–629.

[8]Leibovich, S., "Vortex Stability and Breakdown: Survey and Extension," *AIAA Journal,* Vol. 22, No. 9, 1984, pp. 1192–1206.

[9]Delery, J., Horowitz, E., Leuchter, O., and Solignac, J. L., "Fundamental Studies on Vortex Flows," *La Recherche Aerospatiale* (English ed., ISSN 0379-380X), No. 2, 1984, pp. 1–24.

[10]Metwally, O., Settles, G., and Horstman, C., "An Experimental Study of Shock Wave/Vortex Interaction," AIAA Paper 89-0082, Jan. 1989.

[11]Kandil, O. A., Kandil, H. A., and Liu, C. H., "Supersonic Quasi-Axisymmetric Vortex Breakdown," AIAA Paper 91-3311, Sept. 1991.

[12]Copening, G., and Anderson, J., "Numerical Solutions to Three-Dimensional Shock Wave/Vortex Interaction at Hypersonic Speeds," AIAA Paper 89-0674, Jan. 1989.

[13]Zatoloka, V., Ivanyushkin, A. K., and Nikolayev, A. V., "Interference of Vortexes with Shocks in Airscoops. Dissipation of Vortexes," *Fluid Mechanics, Soviet Research,* Vol. 7, No. 4, 1978, pp. 153–158.

[14]Cattafesta, L. N., and Settles, G. S., "Experiments on Shock/Vortex Interaction," AIAA Paper 92-0315, Jan. 1992.

[15]Kalkhoran, I. M., Sforza, P. M., and Wang, F., "Experimental Study of Shock-Vortex Interaction in a Mach 3 Stream," AIAA Paper 91-3270, Sept. 1991.

[16]Hayes, W. D., "The Vorticity Jump Across a Gasdynamic Discontinuity," *Journal of Fluid Mechanics,* Vol. 2, 1957, pp. 595–600 .

[17]Kalkhoran, I. M., and Sforza, P. M., "Airfoil Pressure Measurements During Oblique Shock Wave/Vortex Interaction," AIAA Paper 92-2631, June 1992.

[18]Kalkhoran, I. M., and Sforza, P. M., "Operation and Calibration of Mach 3 Wind Tunnel in the Polytechnic Aerodynamics Laboratory," Polytechnic Univ., Dept. of Aerospace Engineering, POLY AE Rept. 90-3, Brooklyn, NY, Oct. 1990.

[19]Ames Research Staff, "Equations, Tables, and Charts for Compressible Flow," NACA Rept. 1135, 1953.